Journal of Nuclear Medicine, published on November 22, 2019 as doi:10.2967/jnumed.119.231589

Initial studies with 11C-vorozole positron emission tomography detect over-expression of intra-tumoral aromatase in breast cancer

Anat Biegon[1], Kenneth R. Shroyer[2], Dinko Franceschi[1], Jasbeer Dhawan[1], Mouna Tahmi[1], Deborah Pareto[3], Patrick Bonilla[4], Krystal Airola[1], Jules Cohen[5]

1. Dept. Radiology, Stony Brook University School of Medicine NY USA
2. Dept. Pathology, Stony Brook University School of Medicine NY USA
3. Radiology Department, Vall d'Hebron University Hospital, Barcelona, Spain
4. Dept. Obstetrics and Gynecology, Nassau University Medical center NY USA
5. Hematology/Oncology, Stony Brook University School of Medicine NY USA

Address correspondence to:

Anat Biegon PhD

Dept. Radiology

Stony Brook University School of Medicine, Stony Brook NY 11794-2565

Tel: 631 638 8536 fax 631 632 6294 email: anat.biegon@stonbrook.edu

Supported in part by NIH grant 1R01CA195506-01 (Cohen&Biegon MPI).

Running title: Aromatase imaging in breast cancer

ABSTRACT

Introduction: Aromatase inhibitors are the mainstay of hormonal therapy in estrogen receptor positive breast cancer, although response rate is just over 50% and In vitro studies suggest only two thirds of postmenopausal breast tumors overexpress aromatase. The goal of the present study was to validate and optimize positron emission tomography (PET) with 11C-vorozole for measuring aromatase expression in postmenopausal breast cancer *in vivo*. **Methods:** Ten newly diagnosed, postmenopausal women with biopsy confirmed breast cancer were administered 11C-vorozole intravenously and PET emission data collected between 40 – 90 minutes post-injection. Tracer injection and scanning were repeated 2 hours after ingestion of 2.5mg letrozole p.o. Mean and maximal standard uptake values and ratios to non-tumor tissue (SUVs, SUVRs) were at baseline and after letrozole. Biopsy specimens from the same tumors were stained for aromatase using immunohistochemistry and evaluated for stain intensity and the percentage of immune-positive cells. **Results:** Seven of the 10 women (70%) demonstrated increased mean focal uptake of tracer (SUVR>1.1) coinciding with the mammographic location of the lesion while the other 3 women (30%) did not (SUVR $\leq$1.0). All of the cases with SUVR above 1.1 had mean SUVs above 2.4 and there was no overlap (SUVR$\leq$1, mean SUV from 0.8 to 1.8). SUVR relative to breast around tumor was indistinguishable from the ratio to contralateral breast. Pretreatment with letrozole reduced tracer uptake in the majority of subjects; although the %blocking varied across and within tumors. Tumors with high SUV *in vivo* also showed high immunohistochemical staining intensity. **Conclusion:** PET with 11C-vorozole is a useful technique for measuring aromatase expression in individual breast lesions, enabling a non-invasive quantitative measurement of baseline and post-treatment aromatase availability in primary tumors and metastatic lesions.

Key words: Aromatase, cyp19A, breast cancer, PET, vorozole

INTRODUCTION

Aromatase, a member of the cytochrome P450 protein superfamily, is a unique gene product of the CYP19 gene (*1*). Aromatase catalyzes the last and obligatory step of estrogen biosynthesis. Aromatase expression and activity in the ovary (*2*) support estrogen synthesis for the classical endocrine model, but aromatase and additional enzymes and translocators necessary for local synthesis are also found in classical estrogen target organs such as breast, brain, bone and adipose tissue (*3-6*). Local synthesis and utilization of estrogen ("intracrinology") appears to be the dominant mode of estrogenic function in postmenopausal women (*7*), and there is increasing evidence that a significant proportion of postmenopausal breast tumors (~60%) overexpress aromatase independently of tumor histology and receptor status and are capable of synthesizing and utilizing estrogen through this mechanism, with intra-tumoral estrogen concentration up to an order of magnitude higher than plasma or benign breast level (*8-13*). . Recent studies in animal models suggest overexpression of aromatase is even more important than dysregulated estrogen receptor (ERalpha) expression in the generation of mammary hyperplasia and cancer (*14*).

Although aromatase inhibitors (AI) are among the most effective drugs currently used in the endocrine treatment of breast cancer, for reasons that are not fully understood the objective response rate is about 50% and predictors of responsiveness remain the subject of intense research and debate (15-*22*).

We have recently shown that 11C-vorozole PET is a safe, sensitive and selective non-invasive method for detection of physiological aromatase expression in healthy human subjects (*5*) (*23-26*) First labeled and used in rat and rhesus (*27,28*), a modified synthesis was later introduced, validated and characterized in baboon (*29-31*) and human(*32,33*)brain (Supplemental information 1). The present studies were undertaken in order to validate the use of this technique for the identification of aromatase-overexpressing breast tumors. A new tool for the noninvasive identification of aromatase overexpression in breast cancer may help select appropriate

candidates for AI treatment and prevent unnecessary exposure to the adverse effects of AI, such as joint pain, hot flashes and bone loss (*19*).

MATERIALS AND METHODS

Subjects: Between April 2015 and November 2016, 12 newly diagnosed, postmenopausal women with breast cancer were prospectively recruited from the Carol Baldwin Breast Cancer Center at Stony Brook Medicine for a breast imaging study with 11C-vorozole. Subjects were considered eligible if they were/had 1) postmenopausal (50 years of age or over and at least 12 months from last menstrual period), 2) biopsy-confirmed breast cancer, 3) mammography performed within 3 months of study enrollment, and 4) able to provide written informed consent. Subjects were excluded for: 1) current or past treatment with aromatase inhibitors, 2) current or recent use of hormone replacement therapy, 3) medical conditions likely to affect radiotracer uptake and image interpretation, including cardiovascular disease, breast surgery and breast inflammation/infection, or 4) active smoking. Smokers were excluded since our published findings indicate that tobacco alkaloids inhibit aromatase *in vivo* (*5,31*).

The relevant institutional review boards (IRB and RDRC) of both institutions approved this study and all subjects signed a written informed consent.

PET studies

Radiosynthesis was performed at Weill Cornell Biomedical Imaging Center (CBIC) using published methodology (*29-33*). Intravenous catheters were placed in both arms, one for radiotracer injection and the other for blood sampling.

Patients were placed in the prone position on adjustable 2-piece foam cushion sets available in three sizes, allowing for a customized opening for the breasts to rest in a neutral position.

PET scanning was performed on a Siemens Biograph mCT–S 64 slice PET/CT time of flight tomograph situated at the Weil Cornell Medical College imaging center, in 3D dynamic acquisition mode. A short (<1min) non-diagnostic CT was obtained first for the purpose attenuation correction.

11C-vorozole was injected as a fast, intravenous bolus. Radiochemical purity exceeded 99% and the specific activity ranged from 72 to 185MBq/micromole. The resulting injected mass was less than 1.7 micrograms/study and the radioactive dose ranged from 148 to 296MBq.

Forty minutes post injection, Dynamic PET image acquisition commenced and continued for 50 minutes (5 frames x10 min duration). At the end of the first scan, subjects were given an oral dose of letrozole (2.5mg, Supplemental text 1) and a 2nd injection of tracer was administered 2 hours later, followed by a 2nd CT and PET acquisition ("blocking" study).

PET images were reconstructed using the manufacturer's recommended method for this scanner (TrueX+TOF, ultraHD-PET) consisting of an iterative reconstruction algorithm (2 iterations, 21 subsets), with both attenuation and scatter correction, with a final image size of 200x200 pixels and a voxel size of 4.07x4.07x3mm^3.

PET data analysis was performed by a person (DP, PhD, experienced PET and MRI biomedical physicist) blinded to the identity of the subject and the results of the mammography; using the PMOD program (PMOD technologies LLC, Zurich, Switzerland). The regions of interest were manually delimited with a free-hand tool. A region of interest was placed around the apparent location of the lesion, and similar sized ROIs were also placed in the area adjacent to the lesion and in a similar anatomical location in the contralateral breast. In addition, we measured SUV in the whole contralateral breast. ROI size varied with the size of the individual tumors and breasts. Mean and maximal SUV were calculated using the formula SUV=activity in ROI per cc / injected activity / subject weight in Kg. Subjects were encouraged to report any

adverse effects. In addition, the study coordinator called each subject within 24 hours of the last scan and inquired about adverse effects.

Pathology

Histological typing, tumor grade, tumor stage, ER/PR, HER2 and Ki67 status were determined as per standard methodology in place in the Diagnostic Histology Laboratory of the Department of Pathology. Cut-off values for ER and PR were ≥1% of tumor cells (*34*). HER2 IHC test results of 3+ were scored positive as per HercepTestTM Interpretation Manual (Dako) (*35*). HER2 test results of 2+ were scored as equivocal and prompted FISH testing where a ratio of HER2 copy number to CEP17 control > 2.0 was considered positive.

Aromatase immunohistochemistry

At least 2 slides from each patient specimen, containing tumor and adjacent benign breast tissue, were processed for aromatase immunohistochemistry (IHC) using a goat-anti-human polyclonal antibody to aromatase from Lifespan biosciences, Inc. (Seatle, WA) which has been shown in to produce high quality staining (*11*). The tissue preprocessing and staining protocol was optimized through adaptations of the manufacturer's protocol (Supplemental Fig. 1 and legend).

IHC data analysis

An experienced pathologist (KRS) reviewed the entire section at a magnification of x100 and estimated the percentage of aromatase-positive tumor cells and the staining intensity, which ranged from 0 (negative) to 3 (high intensity).

In addition, digital photographs of stained slides (x400 magnification) were subjected to quantitative analysis using unbiased stereological principles (Supplemental Fig. 1 legend).

Statistics

Statistical analyses were performed using Statview software (Abacus). Analysis of variance was used to examine the effects of diagnostic group, region of interest or time on tracer uptake or immunohistochemical parameters. Analyses yielding a significant main effect were followed by Fisher's PLSD post-hoc analysis with alpha preset at 0.05.

RESULTS

Subject disposition: The first of the 12 consented subjects was not scanned due to a radiosynthesis failure, the eighth was not scanned due to a scheduling failure, and one subject (no. 9, Supplemental Table 1) only received a single (baseline) scan due to injection failure (collapsed vein) in the post-letrozole (blocking) study. Thus, 10 women had baseline scans with 11C-vorozole and 9 had both baseline and blocking studies. Venous blood collection for kinetics and metabolite analysis was attempted but not completed in the majority of subjects due to technical reasons (poor veins, equipment problems).

Patients ranged from 54-75 years old (median age 63) and weighed between 59-113 kg (median weight 79 kg). Six patients had invasive ductal carcinoma, three had invasive lobular carcinoma (2 classic type, 1 pleomorphic) and one patient had mixed ductal/lobular histology. Eight patients had early-stage breast cancer (stage I-III) and 2 had metastases to distant organs (stage IV). Seven patients were ER-positive and 3 patients were ER-negative. Four patients were HER2 positive (Supplemental Table 1).

There were no adverse effects (e.g. Flushing, itching, injection site reaction) reported or observed in any of the 10 participants and 19 scans in this study.

Visual inspection of the 11C-vorozole PET images (averaged emission data collected between 40 - 90 minutes post tracer administration) revealed three distinct profiles (Fig. 1). In 6 out of 10 patients, high focal uptake was observed at baseline, localized to the mammographic location of the tumor (arrow); which was decreased in tumor as well as heart following letrozole

administration (Fig. 1A). Three of the 10 patients did not have focal increase in uptake at the tumor location (Fig. 1B). One patient with highly metastatic cancer had high though heterogeneous focal uptake at the location of the primary tumor ("node 1" arrow points to the area corresponding to the lesion identified on mammography, Fig. 1D). Multiple bone metastases as well as a high uptake area adjacent to the primary tumor (node 2) were observed in the same patient (Fig. 1C and 1D). Letrozole administration did not result in appreciable decrease in uptake in this patient.

PET data analysis in non-tumor regions showed similar mean SUVs in the whole contralateral breast, perilesional breast (tissue around the tumor) and an area in the contralateral breast corresponding in location and size to the primary tumor (mean$\pm$SD: 1.89$\pm$0.5, 1.87$\pm$0.53, 1.9$\pm$0.48 respectively). In 7/10 (70%) of the 10 women scanned, mean SUV in the area coinciding with the mammographic location of the lesion was increased by 10% or more relative to perilesional and contralateral breast ROIs (SUVR>1.1, Fig. 1, I Table 1). The other three women (30%) did not show increased uptake in the tumor (SUVR $\leq$1.0). All of the cases with SUVR above 1.1 had SUVs above 2.4 and there was no overlap in SUV between the two groups (Table 1), with mean SUV in tumors overexpressing aromatase (SUVR>1.1) ranging from 2.47 to 13.6, while the mean SUV of tumors not overexpressing aromatase (SUVR$\leq$1) ranged from 0.8 to 1.8. SUVR relative to breast around tumor was indistinguishable from the ratio to contralateral breast [mean$\pm$SD (range) 2.17$\pm$ 1.66 (0.74-5.8) and 2.08$\pm$1.57 (0.74-5.5) respectively].

Of the 9 women rescanned after a single oral dose of letrozole, measurable blocking of tracer uptake (ranging from 3 to 53% of baseline), indicative of saturable and specific tracer binding, was observed in 7.

In addition, SUVs of the whole contralateral breast from patients were compared to values from a group of 5 healthy postmenopausal volunteers (age 57.8±4.9 years) whose breasts were scanned under a previous protocol using the same tracer and conditions (*5*). Tracer uptake in the breast contralateral to an aromatase positive lesion was significantly higher than uptake in breasts of subjects without breast cancer (Fig. 2), while SUV values in breasts contralateral to tumors not overexpressing aromatase were in between the two groups and not statistically significantly different from either (Fig. 2).

Finally, mean SUVs were compared across frames and frame combinations to assess the feasibility of shortening acquisition time in future clinical studies. Mean SUV was stable between 40 and 90 minutes post injection such that a 20 minute acquisition period between 40 and 60 minutes was sufficient to predict SUV over the maximal acquisition period (up to 90 min) dictated by the tracer half-life (Fig. 3).

Immunohistochemistry

Using our optimized protocol, staining for aromatase gave a consistently high signal in placenta (positive control); with varying intensity in archival tumor and normal tissue specimens. There was no staining when the first antibody was omitted (Supplemental Fig. 1).

Biopsy specimens from aromatase overexpressing tumors showed more staining (%positive multiplied by intensity) with IHC relative to those which did not overexpress aromatase (Fig. 4, supplemental Table 2). When the patient group was split around the median value of SUV and we compared the percentage of aromatase positive cells and the average staining density between the resulting “low” and “high” 11C-vorozole uptake group, there was a statistically significant difference in mean stain density between the high and low groups; while the difference in the percentage of aromatase-positive cells did not reach statistical significance (Fig. 5,

Supplemental Table 2). These findings suggest that increased aromatase expression per cell is a major contributor to the increased PET signal.

DISCUSSION

The primary goal of this study was to validate and optimize the use of 11C-vorozole PET in the non-invasive detection of aromatase-overexpressing tumors in a clinical breast cancer population before and after AI administration.

11C-vorozole PET scans demonstrated increased focal uptake in the affected breast corresponding to the mammographic location of the primary tumor in 7/10 patients. The proportion of 11C-vorozole-overexpressing tumors is in good agreement with published studies of tissue specimens reporting approximately two thirds of postmenopausal breast tumors have increased aromatase expression and activity relative to healthy breast tissue (*3,9-11,13*). Tumor SUVs in these patients were also significantly higher than values obtained in healthy women (*5*), with no overlap. As expected from the literature (*3,9-11,13*); aromatase overexpression could not be predicted from any of the clinicopathological markers routinely evaluated in breast cancer, including tumor type, stage, ER/PR/HER2 expression, or proliferation rate (Ki67).

Interestingly, tracer uptake in the unaffected (contralateral) breast of breast cancer patients was higher than that observed in healthy women suggesting aromatase overexpression in non-tumor tissue may be associated with increased risk of breast cancer.

The two patients with no measurable blocking include the patient with the lowest SUV in this cohort, and one with a high-grade metastatic disease who had the highest SUV in the group. There are several different, potential reasons for the lack of inhibition in an individual patient, including accelerated metabolism or poor bioavailability of the blocking agent, genetic factors or tumor-specific modifications of the aromatase enzyme (*36-40*). Interestingly, the patient with high

SUV was put on neoadjuvant AI and died 6 months after the scan, supporting the notion that aromatase overexpression alone might be necessary but not sufficient to predict responsiveness to AI therapy (*40*); which also requires target engagement by the drug at the planned dose. The remaining study participants were not subsequently treated with aromatase inhibitors prior to resection of their primary breast tumor.

The results of our study, including the feasibility of obtaining meaningful data within a relatively short and convenient acquisition window (40-60 min post injection) suggest PET with 11C-vorozole is a novel, unique and useful technique for characterizing individual breast lesions, enabling, for the first time, a non-invasive quantitative measurement of aromatase availability before and after AI exposure in primary and metastatic lesions. To date, available methods of assessing aromatase expression, including immunohistochemistry (IHC), *in situ* hybridization and enzyme activity assays, require material obtained postmortem or through invasive procedures. IHC is semi-quantitative at best and is usually performed on limited material, such that false negative results are likely, due to partial representation and tumor heterogeneity, as previously discussed in relation to estrogen receptor imaging with 18F-Fuoroestradiol (*41*).

Other PET tracers are currently used in clinical and research settings for breast cancer, most notably 18F-Fluorodeoxyglucose and 18F-fluoroestradiol (FES) (*41-48*). The main advantage of PET over immunohistochemistry of biopsy specimens is that it provides quantitative *in vivo* assessment of all tumor sites throughout the body, an advantage shared by 11C-vorozole. However neither 18F-FDG (*49,50*) nor FES can provide direct information about the expression of intratumoral aromatase, which is increasingly implicated in the etiology, progression, and treatment of breast cancer (*3,9,10,14,36-40*)

The non-invasive nature of the procedure and the short half-life of the isotope also mean that 11C-vorozole PET can be used repeatedly within the same day, enabling efficient clinical or

investigational evaluation of target engagement and pharmacokinetics for novel and established AIs. The procedure can also be repeated periodically during the course of the disease, affording unprecedented access to long term changes in aromatase expression in response to treatment and tumor evolution (*36-40*).

Our study does have limitations, including the small size of the cohort and the limited number of health centers which produce Carbon-11 labeled radiopharmaceuticals. The only other aromatase tracer recently validated in healthy human subjects, 11C-cetrozole (*51*), shares the same limitation. In addition, the study design, including cohort size and composition, does not fully address the possible contribution of 11C-vorozole PET as a clinical companion diagnostic or predictor of AI treatment outcome. In this regard, our ongoing studies include investigation of 11C-vorozole uptake and blocking in a cohort of patients with metastatic disease who also had 18F-FDG and MRI scans performed as part of their clinical workup. Future directions include testing the relationship between tumor response to AIs and pre-treatment aromatase expression and blocking with commonly used AI given for a slightly longer period (up to 2 weeks, to ensure steady state) (*52*) which will also include measurement of individual AI plasma levels, relevant polymorphisms in the aromatase gene (*36*) as well as the development and validation of AI diagnostic and theranostic radiopharmaceuticals labeled with isotopes with a longer half-life than Carbon-11 (*53*).

CONCLUSION

PET with 11C-vorozole is a useful technique for measuring aromatase expression in individual breast lesions, enabling a non-invasive quantitative measurement of baseline and post-treatment aromatase availability in primary and metastatic lesions, which can be used to enhance tumor characterization, patient selection and treatment monitoring in breast cancer.

Financial disclosure: Supported by NIH grant 1R01CA195506-01 (Cohen&Biegon MPI)

No potential conflicts of interest relevant to this article exist.

ACKNOWLEDGMENTS: The authors thank Drs. Alison Stopeck and Leah Baer of Stony Brook Medicine for help with subject recruitment, William Scherl for study coordination, Shankar Vallabhajosula PhD and staff at the Citigroup Biomedical Imaging Center (CBIC) for tracer production and scan execution.

KEY POINTS

QUESTION: Is it possible to non-invasively visualize and measure aromatase availability in breast tumors *in vivo*?

PERTINENT FINDINGS: PET with [^{11}C]vorozole detected high focal uptake coinciding with mammographic tumor location in seven breast cancer patients. Biopsy material from all of these tumors demonstrated high density of aromatase immunohistochemical staining relative to 3 tumors which did also did not have high focal uptake of radiotracer.

IMPLICATIONS FOR PATIENT CARE: PET with [^{11}C]vorozole can be used to improve tumor characterization, treatment planning and treatment monitoring in women with breast cancer considering hormonal treatment with aromatase inhibitors.

REFERENCES

1. Danielson P. The cytochrome P450 superfamily: biochemistry, evolution and drug metabolism in humans. *Curr drug metabolism.* 2002;3:561-597.

2. Kragie L. Aromatase in primate pregnancy: a review. *Endocr Res.* 2002;28:121-128.

3. Brodie A, Lu Q, Nakamura J. Aromatase in the normal breast and breast cancer. *J Steroid Biochem Mol Biol.* 1997;61:281-286.

4. Simpson ER, Clyne C, Rubin G, et al. Aromatase—a brief overview. *Annu Rev Physiol.* 2002;64:93-127.

5. Biegon A, Alexoff DL, Kim SW, et al. Aromatase imaging with [N-methyl-11C] vorozole PET in healthy men and women. *J Nucl Med.* 2015;56:580-585.

6. Rone MB, Fan J, Papadopoulos V. Cholesterol transport in steroid biosynthesis: role of protein–protein interactions and implications in disease states. *Biochim Biophys Acta Mol Cell Biol Lipids.* 2009;1791:646-658.

7. Labrie F. All sex steroids are made intracellularly in peripheral tissues by the mechanisms of intracrinology after menopause. *J Steroid Biochem Mol Biol.* 2015;145:133-138.

8. McNamara KM, Sasano H. The intracrinology of breast cancer. *J Steroid Biochem Mol Biol.* 2015;145:172-178.

9. Lu Q, Nakmura J, Savinov A, et al. Expression of aromatase protein and messenger ribonucleic acid in tumor epithelial cells and evidence of functional significance of locally produced estrogen in human breast cancers. *Endocrinology.* 1996;137:3061-3068.

10. Di G, Lu J, Song C, Li H, Shen Z, Shao Z. Over expression of aromatase protein is highly related to MMPs levels in human breast carcinomas. *J Exp Clin Cancer Res.* 2005;24:601-607.

11. Singer CF, Fink-Retter A, Gschwantler-Kaulich D, et al. Selective spatial upregulation of intratumoral stromal aromatase in breast cancer patients: evidence for imbalance of local estrogen metabolism. *Endocr Relat Cancer.* 2006;13:1101-1107.

12. Bulun SE, Simpson ER. Aromatase expression in women's cancers. *Innovative Endocrinology of Cancer*: Springer; 2008:112-132.

13. Geisler J, Suzuki T, Helle H, et al. Breast cancer aromatase expression evaluated by the novel antibody 677: correlations to intra-tumor estrogen levels and hormone receptor status. *J Steroid Biochem Mol Biol.* 2010;118:237-241.

14. Díaz-Cruz ES, Sugimoto Y, Gallicano GI, Brueggemeier RW, Furth PA. Comparison of increased aromatase versus ERα in the generation of mammary hyperplasia and cancer. *Cancer Res.* 2011;71:5477-5487.

15. Cohen MH, Johnson JR, Li N, Chen G, Pazdur R. Approval summary: letrozole in the treatment of postmenopausal women with advanced breast cancer. *Clin Cancer Res.* 2002;8:665-669.

16. Iveson T, Smith I, Ahern J, Smithers D, Trunet P, Dowsett M. Phase I study of the oral nonsteroidal aromatase inhibitor CGS 20267 in healthy postmenopausal women. *J Clin Endocrinol Metab.* 1993;77:324-331.

17. Buzdar AU, Robertson JF, Eiermann W, Nabholtz JM. An overview of the pharmacology and pharmacokinetics of the newer generation aromatase inhibitors anastrozole, letrozole, and exemestane. *Cancer.* 2002;95:2006-2016.

18. Santen R, Yue W, Naftolin F, Mor G, Berstein L. The potential of aromatase inhibitors in breast cancer prevention. *Endocr Relat Cancer.* 1999;6:235-243.

19. Smith IE, Dowsett M. Aromatase inhibitors in breast cancer. *N Engl J Med.* 2003;348:2431-2442.

20. Regan MM, Neven P, Giobbie-Hurder A, et al. Assessment of letrozole and tamoxifen alone and in sequence for postmenopausal women with steroid hormone receptor-positive breast cancer: the BIG 1-98 randomised clinical trial at 8· 1 years median follow-up. *Lancet Oncol.* 2011;12:1101-1108.

21. Miron L, Negura L, Peptanariu D, Marinca M. Research on aromatase gene (CYP19A1) polymorphisms as a predictor of endocrine therapy effectiveness in breast cancer. *Rev Med Chir Soc Med Nat Iasi.* 2012;116:997-1004.

22. Moy I, Lin Z, Rademaker AW, Reierstad S, Khan SA, Bulun SE. Expression of estrogen-related gene markers in breast cancer tissue predicts aromatase inhibitor responsiveness. *PLoS One.* 2013;8:e77543.

23. Bossche HV, Willemsens G, Roels I, et al. R 76713 and enantiomers: selective, nonsteroidal inhibitors of the cytochrome P450-dependent oestrogen synthesis. *Biochem Pharmacol.* 1990;40:1707-1718.

24. Koymans LM, Moereels H, Bossche HV. A molecular model for the interaction between vorozole and other non-steroidal inhibitors and human cytochrome P450 19 (P450 aromatase). *J Steroid Biochem Mol Biol.* 1995;53:191-197.

25. Johnston SR, Smith IE, Doody D, Jacobs S, Robertshaw H, Dowsett M. Clinical and endocrine effects of the oral aromatase inhibitor vorozole in postmenopausal patients with advanced breast cancer. *Cancer Res.* 1994;54:5875-5881.

26. de Jong PC, van de Ven J, Nortier HW, et al. Inhibition of breast cancer tissue aromatase activity and estrogen concentrations by the third-generation aromatase inhibitor vorozole. *Cancer Res.* 1997;57:2109-2111.

27. Lidström P, Bonasera TA, Kirilovas D, et al. Synthesis, in vivo rhesus monkey biodistribution and in vitro evaluation of a 11C-labelled potent aromatase inhibitor:[N-methyl-11C] vorozole. *Nucl Med Biol.* 1998;25:497-501.

28. Takahashi K, Bergström M, Frändberg P, Vesström E-L, Watanabe Y, Långström B. Imaging of aromatase distribution in rat and rhesus monkey brains with [11C] vorozole. *Nucl Med Biol.* 2006;33:599-605.

29. Kim SW, Biegon A, Katsamanis ZE, et al. Reinvestigation of the synthesis and evaluation of [N-methyl-11C] vorozole, a radiotracer targeting cytochrome P450 aromatase. *Nucl Med Biol.* 2009;36:323-334.

30. Pareto D, Biegon A, Alexoff D, et al. In vivo imaging of brain aromatase in female baboons:[11C] vorozole kinetics and effect of the menstrual cycle. *Mol Imaging.* 2013;12:7290.2013. 00068.

31. Biegon A, Kim S-W, Logan J, Hooker JM, Muench L, Fowler JS. Nicotine blocks brain estrogen synthase (aromatase): in vivo positron emission tomography studies in female baboons. *Biol Psychiatry.* 2010;67:774-777.

32. Biegon A, Kim SW, Alexoff DL, et al. Unique distribution of aromatase in the human brain: In vivo studies with PET and [N-methyl-11C] vorozole. *Synapse.* 2010;64:801-807.

33. Logan J, Kim SW, Pareto D, et al. Kinetic analysis of [11C] vorozole binding in the human brain with positron emission tomography. *Mol Imaging.* 2014;13:7290.2014. 00004.

34. Yi M, Huo L, Koenig KB, et al. Which threshold for ER positivity? A retrospective study based on 9639 patients. *Ann Oncol.* 2014;25:1004-1011.

35. Dako. HercepTestTM Interpretation Manual Breast Cancer. Agilent Technologies; 2014. Accessed date: September 9, 2019.

36. Garcia-Casado Z, Guerrero-Zotano A, Llombart-Cussac A, et al. A polymorphism at the 3'-UTR region of the aromatase gene defines a subgroup of postmenopausal breast cancer patients with poor response to neoadjuvant letrozole. *BMC Cancer.* 2010;10:36.

37. Catalano S, Giordano C, Panza S, et al. Tamoxifen through GPER upregulates aromatase expression: a novel mechanism sustaining tamoxifen-resistant breast cancer cell growth. *Breast Cancer Res Treat.* 2014;146:273-285.

38. Milosevic J, Klinge J, Borg A-L, Foukakis T, Bergh J, Tobin NP. Clinical instability of breast cancer markers is reflected in long-term in vitro estrogen deprivation studies. *BMC Cancer.* 2013;13:473.

39. Shibahara Y, Miki Y, Ishida T, et al. Immunohistochemical analysis of aromatase in metastatic lymph nodes of breast cancer. *Pathol Int.* 2013;63:20-28.

40. de Jong PC, Blankenstein MA, Nortier JW, et al. The relationship between aromatase in primary breast tumors and response to treatment with aromatase inhibitors in advanced disease. *J Steroid Biochem Mol Biol.* 2003;87:149-155.

41. Peterson LM, Mankoff DA, Lawton T, et al. Quantitative imaging of estrogen receptor expression in breast cancer with PET and 18F-fluoroestradiol. *J Nucl Med.* 2008;49:367-374.

42. Kumar R, Lal N, Alavi A. 18F-FDG PET in detecting primary breast cancer. *J Nucl Med.* 2007;48:1751-1751.

43. Çermik TF, Mavi A, Basu S, Alavi A. Impact of FDG PET on the preoperative staging of newly diagnosed breast cancer. *Eur J Nucl Med Mol Imaging.* 2008;35:475-483.

44. Basu S, Chen W, Tchou J, et al. Comparison of triple-negative and estrogen receptor-positive/progesterone receptor-positive/HER2-negative breast carcinoma using quantitative fluorine-18 fluorodeoxyglucose/positron emission tomography imaging parameters. *Cancer.* 2008;112:995-1000.

45. Lakhani P, Maidment AD, Weinstein SP, Kung JW, Alavi A. Correlation between Quantified Breast Densities from Digital Mammography and 18F-FDG PET Uptake. *Breast J.* 2009;15:339-347.

46. Kumar R, Alavi A. Fluorodeoxyglucose-PET in the management of breast cancer. *Radiol Clin North Am.* 2004;42:1113-1122.

47. Lerman H, Metser U, Grisaru D, Fishman A, Lievshitz G, Even-Sapir E. Normal and abnormal 18F-FDG endometrial and ovarian uptake in pre-and postmenopausal patients: assessment by PET/CT. *J Nucl Med.* 2004;45:266-271.

48. Liao GJ, Clark AS, Schubert EK, Mankoff DA. 18F-Fluoroestradiol PET: current status and potential future clinical applications. *J Nucl Med.* 2016;57:1269-1275.

49. Mortimer JE, Dehdashti F, Siegel BA, Trinkaus K, Katzenellenbogen JA, Welch MJ. Metabolic flare: indicator of hormone responsiveness in advanced breast cancer. *J Clin Oncol.* 2001;19:2797-2803.

50. Mankoff DA, Dunnwald LK, Gralow JR, et al. Blood flow and metabolism in locally advanced breast cancer: relationship to response to therapy. *J Nucl Med.* 2002;43:500-509.

51. Takahashi K, Hosoya T, Onoe K, et al. 11C-cetrozole: an improved C-11C-methylated PET probe for aromatase imaging in the brain. *J Nucl Med.* 2014;55:852-857.

52. Pfister CU, Martoni A, Zamagni C, et al. Effect of age and single versus multiple dose pharmacokinetics of letrozole (Femara®) in breast cancer patients. *Biopharmaceutics & drug disposition.* 2001;22:191-197.

53. Erlandsson M KF, Takahashi K, Långström, B. 18F-Labelled vorozole analogues as PET tracer for aromatase. *J Labelled Comp Radiopharm.* 2008;51:207-212.

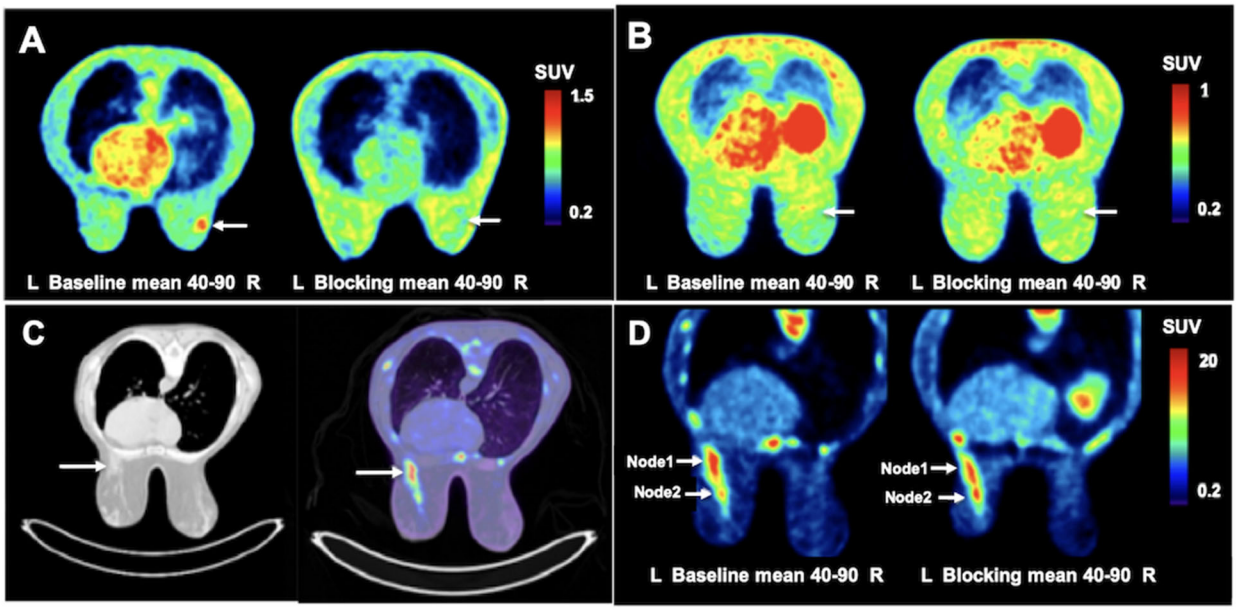

Figure 1. Aromatase availability imaged by 11C-vorozole in women with breast cancer.

A. SUV map from a patient with a single lesion on mammography (arrow) before and after letrozole administration ("blocking"). Note focal uptake in tumor area (arrow) at baseline and decreased uptake in tumor as well as heart. This pattern was observed in six out of 10 patients. B. SUV map from a patient with a single lesion on mammography (arrow) which did not show increased tracer uptake. This pattern was seen in 3 women. C. CT (left) and PET overlayed on CT (right) from a patient with stage 4 metastatic cancer. The arrow indicates the location of the primary tumor on the patient's mammogram. D. SUV maps of same patient. The "node 1" arrow points to the location and size identified on mammography. Multiple bone metastasis as well as a high uptake area adjacent to the primary tumor (node 2) can be seen with no apparent blocking.

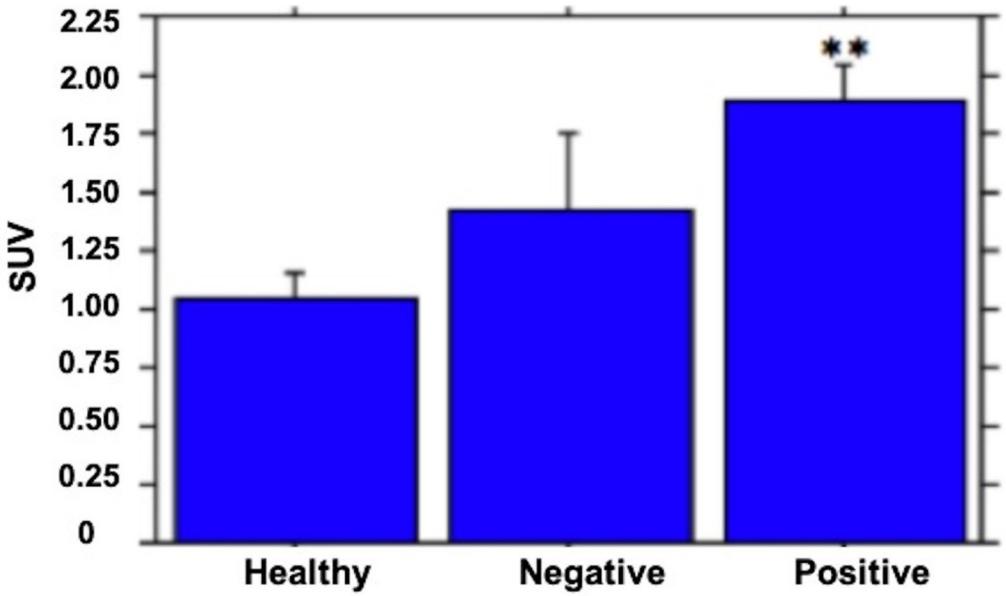

Figure 2. 11C-vorozole uptake in breast tissue contralateral to aromatase-overexpressing and non-overexpressing tumors and breasts of healthy women

Bars depict means and SEM of N subjects/group. One-way ANOVA demonstrated a significant main effect of group ($F=5.94$, $p<0.02$). Fisher's PLSD post hoc test demonstrated a highly significant difference (**$p=0.005$) between healthy breasts (Healthy, N=5) and breasts contralateral to an aromatase overexpressing (Positive, N=7) lesion. Intermediate values, not significantly different form either group, were observed in breast tissue contralateral to aromatase negative (Negative, N=3) lesions.

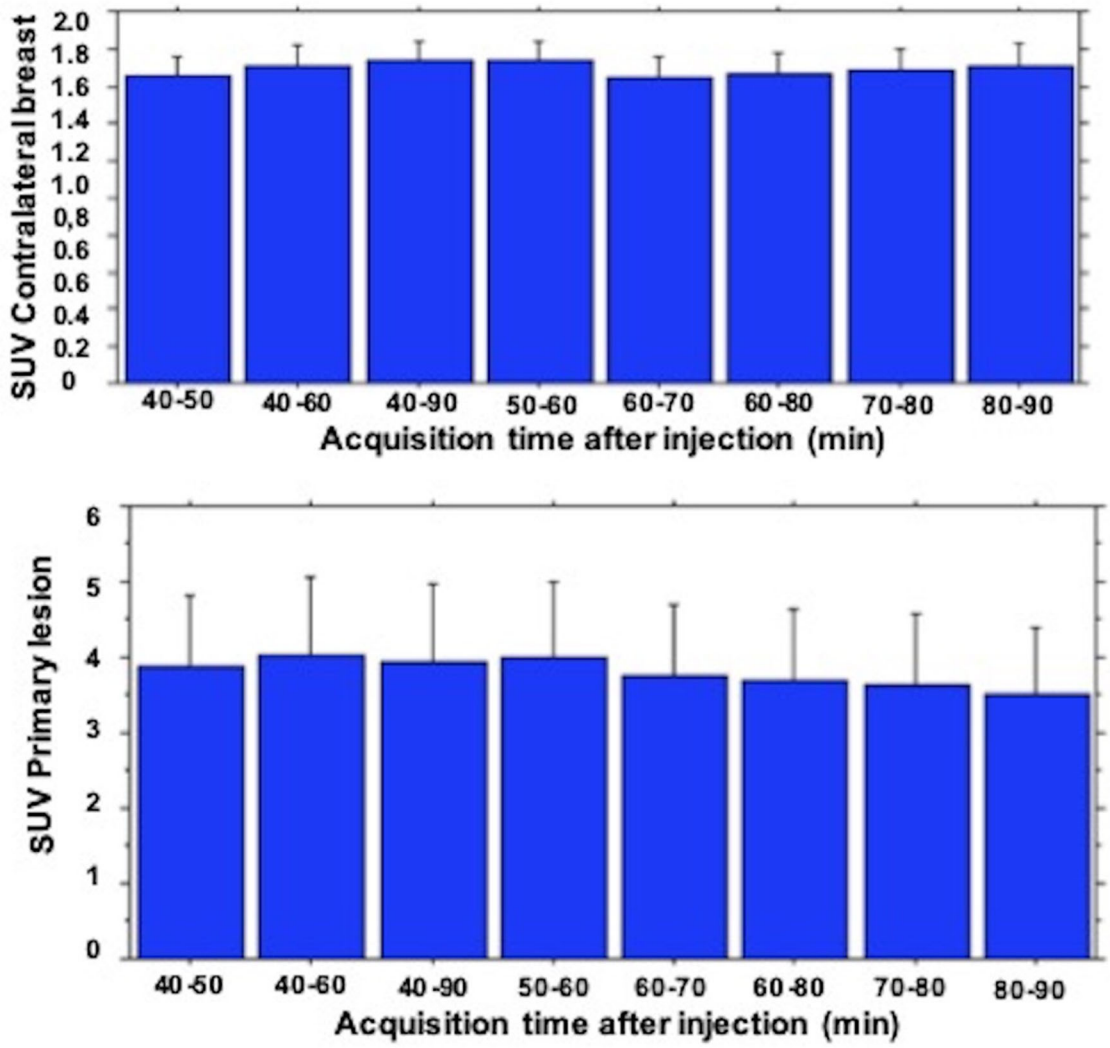

Figure 3. Mean tracer uptake in healthy breast and tumor over various time intervals.

Bars represent means and SEM of 10 subjects (baseline scan).

Emission data acquisition began 40 minutes after tracer injection and continued for 50 minutes.

SUV was averaged over the whole acquisition period (40-90) and several shorter time intervals.

There was no statistically significant difference (one way ANOVA) among the various intervals.

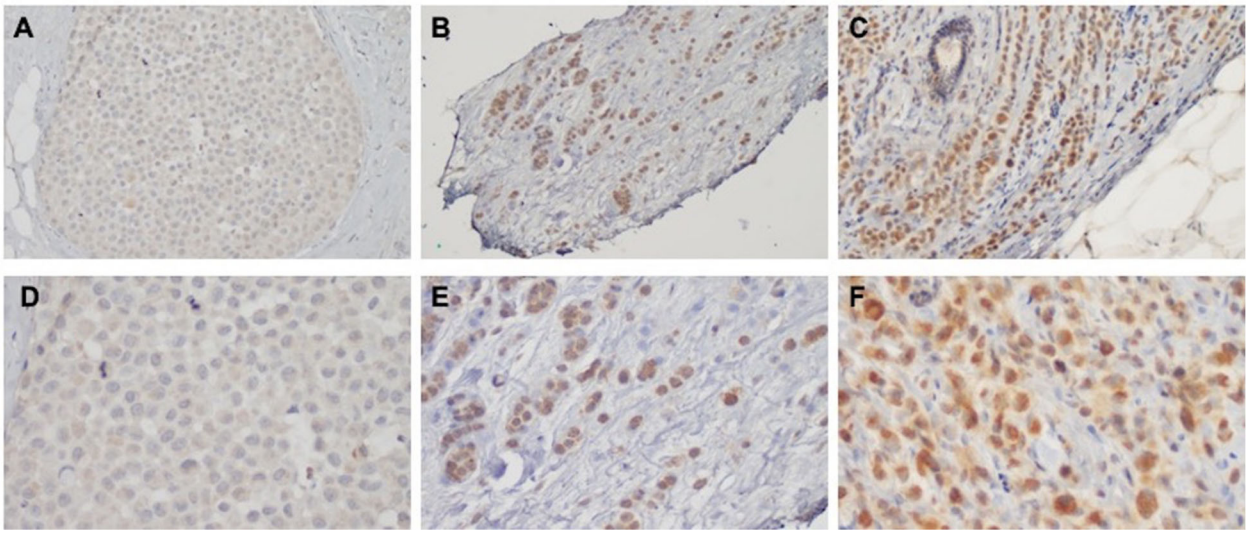

Figure 4. Immunohistochemical staining for aromatase in biopsy material from breast cancer patients imaged with [^{11}C]vorozole *in vivo.*

A,D. Patient with low intensity labeling and low [^{11}C]vorozole uptake. B,E. Patient with moderately high staining intensity and moderately high [^{11}C]vorozole uptake C,F. Patient with high staining intensity and high [^{11}C]vorozole uptake. The top row (A-C) images were magnified x200 and the bottom row (D-F) where obtained at x400 magnification.

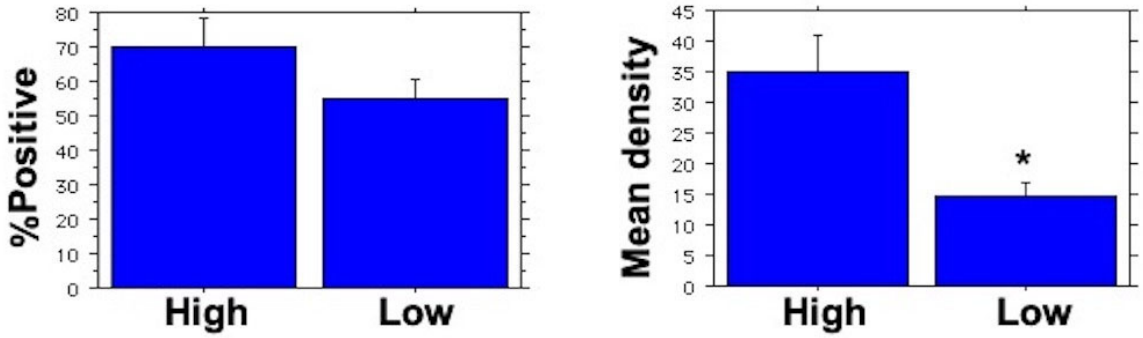

Figure 5. Quantitative immunohistochemical analysis of aromatase expression in patients with high and low vorozole uptake.

Left panel depict the mean percentage of cells positively stained for aromatase among patients with high (above median, N=5) and low (below median, N=5) SUV. Difference was not statistically significant (p=0.2). Right panel shows mean staining intensity (density, 255-grey level) for aromatase among patients with high (above median, N=5) and low (below median, N=5) SUV. *p<0.02 Student's t-test, two tailed.

Table 1. [^{11}C] vorozole uptake in tumor area before and after letrozole

No	Lesion, SUV mean	Lesion, SUV max	%block Mean	SUVR Mean
2	13.69	24.43	0	5.87
3	4.66	6.03	21.8	2.84
4	5.80	7.83	20.1	2.75
5	1.61	3.80	25.7	0.92
6	0.79	1.41	0	1.00
7	3.63	4.86	53.3	1.44
9	2.47	3.03	na	1.91
10	1.78	4.40	3	1.01
11	3.20	4.09	56.3	1.80
12	2.61	3.98	18.9	1.73

SUV mean = mean standard uptake value in the area of the primary lesion, SUV max=maximal SUV value in the same area. %block=100-SUV post letrozole/baseline/0.01. SUVR = ratio of mean SUV in primary lesion over similar area in contralateral breast. na=not available, no blocking study performed.

Supplemental material

Supplemental text 1. Pharmacological proerties of 11C-vorozole and letrozole.

S -Vorozole (6-[(S)-(4-chlorophenyl)-1H-1,2,4-triazol- 1-ylmethyl]-1-methyl-1H-benzotriazole) is a specific and potent (Ki=0.7nM) nonsteroidal, competitive aromatase inhibitor. Originally developed as an anti-neoplastic agent, the compound is extensively metabolized by the liver and has an elimination half-life of 8 hours.

Peak levels in tissue were achieved by 30 minutes followed by stabilization over the 90 minutes acquisition period. Metabolite-corrected plasma levels indicated a plasma half-life of more than 60 minutes (*32*). Kinetic modeling showed similar rank order of target density in various brain regions using several analytical approaches including a single tissue compartment, 2 tissue compartment, Logan plot, tissue over plasma ratios and brain region over cerebellum in primate as well as human brain (*30,33*).

As part of the tracer validation in healthy controls, 33 healthy subjects, 13 men and 20 women, were enrolled in a multiple-scan study, which entailed 2 visits and 4 scans/subject, including combinations of brain, body, retest and blocking studies (*5*). There were no adverse or clinically detectable pharmacologic effects in any of the 33 subjects and more than 100 scans performed.

Letrozole is an FDA approved aromatase inhibitor (brand name Femara™) prescribed for the treatment pf breast cancer patients as an oral daily 2.5mg dose (*15*). Studies performed in healthy volunteers with a single dose of letrozole show that a standard 2.5 mg oral dose blocks close to 80% of aromatase activity and Cmax is reached within 2-2.5 hours. The effect of a single dose of the drug (monitored by decline of estrogen levels) peaks within 2-2.5 hours of administration and lasts for more than 24 hours (*16,17*). Using the same dose and time interval, we have previously shown, as part of the tracer validation process, that letrozole blocks 11C-vorozole brain uptake (*5,29-33*).

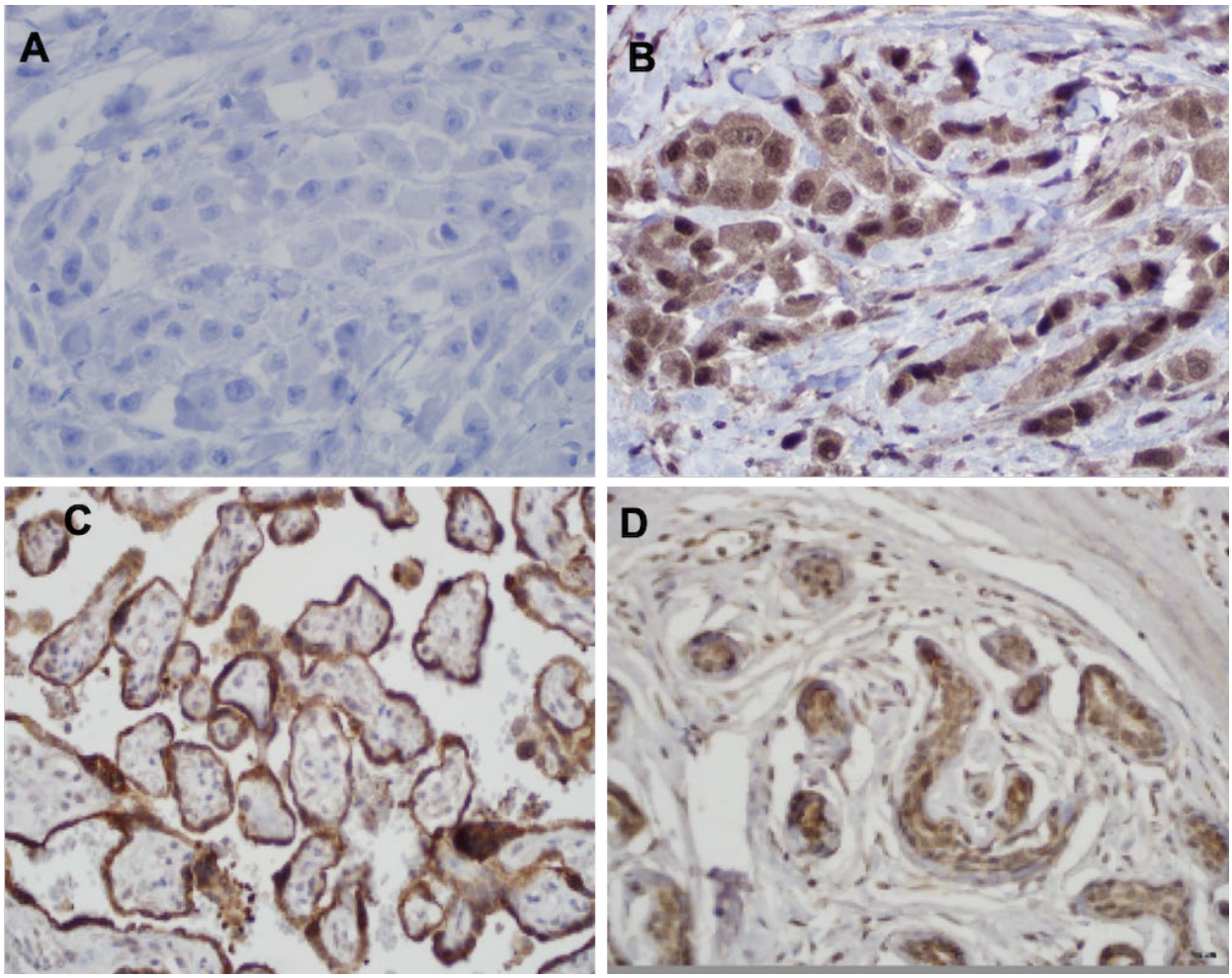

Supplemental Figure 1. Aromatase staining in placenta, healthy breast and breast tumors.

A: Archival breast cancer section processed without primary antibody (negative control). B. Consecutive section from same tumor as A stained with primary antibody to aromatase. C. Positive control showing high levels of aromatase in normal placenta (chorionic villi). D. Low-moderate expression of aromatase in healthy breast ducts and lobules. Original magnification 400x.

Methods: Tissue specimens used for method optimization and validation were obtained under institutional review board approval from the archival collections of formalin-fixed, paraffin-

embedded blocks at the State University of New York at Stony Brook, Department of Pathology between 2004 and 2008.

The tissue pre-processing and staining protocol was adapted from the manufacturer's protocol to maximize signal intensity and specificity (Supplemental Fig. 1) by testing different reagents, temperatures and durations of incubation in the presence as well as in the absence of the primary antibody, first on placenta tissue, known to express high levels of aromatase, and then in normal breast and breast tumor tissue. Subsequently, a positive (human placenta) and negative (primary antibody omitted) control slide were processed in conjunction with each staining experiment

The optimized protocol involved sectioning of tumor and benign breast tissues at 4 um, mounting on charged glass slides (Superfrost Plus), and baking overnight at 60^0C. The slides were deparaffinized in xylene and rehydrated through graded alcohols. Endogenous peroxidase activity was blocked by 5 min treatment with 3.0% hydrogen peroxide and antigen retrieval by heating the slides to 120^oC for 10 min in 20 mM citrate buffer (pH 6.0). The slides were then incubated with aromatase antibody diluted 1:1000 at room temperature for 60 min, followed by visualization using an indirect avidin-biotin–based immunoperoxidase method, using a Vectastain Elite ABC kit. Subsequently, the sections were developed using 3,3' diaminobenzidine (DAB), counterstained with hematoxylin, and then dehydrated in graded alcohols and coverslipped. For each batch, the IHC staining was revalidated using positive and negative controls.

Supplemental Table 1. Clinical demographics of scanned subjects

Subject	Age (years)	Weight (Kg)	Type	*Stage	TNM	Grade	ER	PR	HER2	Ki67
2	69	64	ILC(pleo)	IV	M1	NS	96%	94%	POS	11%
3	60	69	IDC	II	cT2 N1	3	NEG	NEG	POS	31%
4	60	87	IDC	II	cT2 N0	2	95%	5-90%	POS	60%
5	61	88	IDC	I	pT1a N0	1	100%	60%	NEG	5%
6	79	113	ILC	II	cT2 N0	2	80-95%	5-20%	NEG	12-30%
7	64	94	ILC	I	pT1a N0	2	94%	NEG	NEG	10%
9	75	59	IDC& ILC	II	cT2 N1	1-2	95%	10-50%	NEG	8-15%
10	62	71	IDC	IV	M1	2	2-3%	NEG	POS	12-25%
11	54	72	IDC	II	cT2 N0	3	NEG	NEG	NEG	70%
12	73	96	IDC	III	cT1c N2	3	NEG	NEG	NEG	80%

* AJCC Staging system, 7th edition

Abbreviations: ILC = Invasive lobular carcinoma, Pleo = Pleomorphic type, IDC = Invasive ductal carcinoma, IDC and ILC = mixed histology with features of IDC and ILC, TNM = Tumor, Node, Metastasis; c = clinical p = pathologic, m = multifocal

T1 = primary tumor <2 cm in size, T1a = <0.5 cm, T1b = 0.5-1 cm, T1c = 1-2 cm, T2 = 2-5 cm T3 = >5 cm, N0 = no axillary lymph nodes (LN) involved, N1 = 1-3 axillary LN, N2 = 4-10 axillary LN, M1 = presence of distant metastases (i.e. liver, lungs, bone)

NS=not specified ER=estrogen receptor status, PR=progesterone receptor status

NEG=negative POS=positive

Supplemental table 2. Quantification of Immunohistochemical staining for aromatase in breast tumor biopsy samples of scanned subjects

Subject	%all	ODall	%xOD	SUV	%path	Intensity	%xIntensity
2	77.24	46.23	35.71	13.69	100.00	2.00	2.00
3	49.25	43.34	21.34	4.66	100.00	1.00	1.00
4	63.92	32.72	20.91	5.80	80.00	1.00	0.80
5	69.70	26.92	18.76	1.61	100.00	1.00	1.00
6	52	21.19	11.02	0.79	0.00	0.00	0.00
7	60.53	78.79	47.69	3.63	50.00	2.00	1.00
9	35.80	22.96	8.22	2.47	10.00	3.00	0.30
10	56.67	32.36	18.34	1.78	100.00	1.00	1.00
11	98.11	50.00	49.05	3.20	100.00	1.00	1.00
12	60.98	29.02	17.70	2.61	100.00	1.00	1.00

The three columns on the left depict the results of quantitative non-biased cell counts and density measurements performed as described below. The middle column has the mean SUV values from table 1 in the main manuscript. The three columns on the left depict the results of a semi-quantitative pathological examination as described below.

Abbreviations: %all=Aromatase (DAB) positive cells/hematoxylin stained nuclei x 100.

ODall = mean optical density (255-grey level) of all aromatase (DAB) positive cells. %XOD = %all multiplied by ODall. SUV=Mean Standardized Uptake Value of [11C]vorozole in the tumor. %path=Estimate of percentage of malignant cells positive for aromatase.

Intensity=estimate of staining intensity in malignant cells. %Xintensity=percentage of positive malignant cells multiplied by intensity.

Quantitative analysis of stained cells: Digital photographs of stained slides (x400 magnification) were subjected to quantitative analysis using ImageJ (NIH) software. The total number of cells (hematoxylin stained nuclei) and aromatase (DAB) positive cells were counted using unbiased stereological principles (minimum 100 cells, 3 fields). Subsequently, the images

were de-convoluted to separate the DAB signal from the H&E signal and DAB signal density was measured in at least 100 cells/subject to assess changes in aromatase expression per cell.

Semi-quantitative analysis of malignant cells: An experienced pathologist (KRS) reviewed the entire section at a magnification of x100 and scored the percentage of aromatase positive malignant cells (0-100) and the staining intensity on a scale of 0 (none) to 3 (high intensity).